JCTC Journal of Chemical Theory and Computation

Article

pubs.acs.org/JCTC

Exploring Potential Energy Surfaces of Large Systems with Artificial Force Induced Reaction Method in Combination with ONIOM and Microiteration

Satoshi Maeda,*[,†] Erika Abe,[‡] Miho Hatanaka,[‡] Tetsuya Taketsugu,[†] and Keiji Morokuma*[,‡,§]

[†]Department of Chemistry, Faculty of Science, Hokkaido University, Sapporo 060-0810, Japan

[‡]Fukui Institute for Fundamental Chemistry, Kyoto University, Kyoto 606-8103, Japan

[§]Department of Chemistry and Cherry L. Emerson Center for Scientific Computation, Emory University, Atlanta, Georgia 30322, United States

ABSTRACT: Development of efficient methods for finding chemical reaction pathways has been one of the central subjects of theoretical chemistry. Recently, the artificial force induced reaction (AFIR) method enabled automated search for associative reaction pathways between multiple reactant molecules and has been applied to reactions involving a few tens of atoms. To expand its applicability to large systems, we combined it with the geometrical microiteration technique. With this extension, full optimization of transition state structures of enzymatic reactions in the protein became possible within the QM/MM framework. Performance of the microiteration-AFIR method was tested for a single water catalyzed Aldol reaction in $(H_2O)_{299}$ cluster and for an enzymatic reaction of the isopenicillin N synthase, where the potential energy surfaces were calculated by the ONIOM(QM/MM) method. These numerical tests demonstrated that the present method is promising in predicting reaction pathways that take place within an active site (consisting of tens of atoms) in a very large environment such as protein and solution.

1. INTRODUCTION

The mechanism of chemical reaction can be studied theoretically by computing transition state (TS) structures and energies on a potential energy surface (PES) on the basis of quantum chemical calculations. The success of such studies has been greatly supported by a variety of geometry optimization techniques.[1−5] Nowadays, optimization of positions of dozens of atoms can be done routinely. Moreover, the hybrid quantum mechanics (QM)/molecular mechanics (MM) approach[6−11] and the introduction of the geometrical microiteration technique[12,13] enabled full optimization of TS structures for enzymatic reactions involving thousands or more atoms.[14] It should be noted that our focus in the present paper is on local chemical bond rearrangements involving a few to several tens of atoms. Global optimization, conformation sampling, crystal structure sampling, etc.,[15−21] are outside the scope of this paper.

In general, some estimates about reaction mechanisms are required in theoretical studies. Quasi-Newton methods can locate a TS structure when a reasonable initial guess is provided. Interpolation methods can find a reaction path and associated TS(s) between given end points without a guess of TS, although one has to know (or estimate) not only the product(s) but also some key intermediates to find the lowest path when there are multiple pathways. Coordinate driving methods, which can calculate reaction pathways along given reaction variable(s), are often used when all important reaction variables are known. These methods are very useful when required inputs, such as guesses of TSs, product(s), intermediates, and/or reaction variables, are available or can be estimated easily. For more about these methods, see the extensive review by Schlegel.[5]

There are several approaches that can find reaction pathways systematically without any input concerned with reaction mechanisms.[22−26] In particular, the global reaction route mapping (GRRM) method can find all reaction pathways starting from explicit local minima by following anharmonic downward distortion pathways and has been applied to a variety of systems ranging from unimolecular thermal- and photoreactions to molecular clusters and asymmetric catalysis.[27−35] However, these methods are designed to initiate the search starting from local minima and are not necessarily most efficient for associative reactions between several molecules.

Our focus in the present study is finding associative reaction pathways systematically without using any initial guess. This has been enabled by our artificial force induced reaction (AFIR) method.[36] The AFIR method has been applied to a multicomponent reaction,[37] combustion reactions involving multiple PESs,[38] (metal-free) organic reactions,[39] and an organometallic catalysis.[40] In the application to combustion reactions,[38] the seam model function (SMF) approach was used in combination with the AFIR method, and an automated search for minima on seam of crossing (MSXs) between different spin states was introduced. In the present study, we extend the applicability of the AFIR method to large systems by combining with the ONIOM(QM/MM) and geometrical microiteration methods. The present approach was tested for an organic reaction in a model water cluster $(H_2O)_{299}$ and an enzymatic reaction in the protein. In the enzymatic reaction,

Special Issue: Berny Schlegel Festschrift

Received: July 23, 2012
Published: September 1, 2012

performance of the search for MSXs by the SMF-AFIR method was also tested.

2. METHODS

AFIR method. In the AFIR method,[36] reaction pathways between two reactants A and B can be obtained by minimizing the following function, called AFIR function, starting from random or inputted initial orientations between A and B.

$$X(\mathbf{Q}) = E(\mathbf{Q}) + \frac{\gamma}{\left[2^{-1/6} - \left(1 + \sqrt{1 + \frac{\gamma}{\varepsilon}}\right)^{-1/6}\right]R_0} \times \frac{\sum_{i\in A}\sum_{j\in B} r_{ij}\left[\frac{(R_i + R_j)}{r_{ij}}\right]^p}{\sum_{i\in A}\sum_{j\in B}\left[\frac{(R_i + R_j)}{r_{ij}}\right]^p} \quad (1)$$

where $E(\mathbf{Q})$ is the PES that depends on the atomic coordinates $\mathbf{Q} = \{Q_k\}$, r_{ij} is a distance between the ith and jth atoms, summations are taken over all pairs of atoms in A and B, and R_0 and ε are parameters in the Lennard-Jones potential for argon clusters (R_0 = 3.8164 Å and ε = 1.0061 kJ/mol). The model collision energy parameter γ determines the strength of the force and the γ value is automatically adjusted between γ_{MAX} and γ_{MIN}.[39] The inverse distance weighting[41] is employed so that the force is imposed only to closely interacting pairs, where p is a parameter (set to the standard value[36] p = 6) of the weight. In this weight, each inverse distance is scaled by the sum of covalent radii ($R_i + R_j$) of the ith and jth atoms, respectively, to take the difference in atomic size into account. For reactions involving three or more reactants (C, D, ...), one can add terms for A−C, B−C, etc.[39]

As demonstrated in ref 39, the second term in eq 1 emphasizes subtle potential energy dents generated by attractive orbital interactions between given reactants. In other words, maximal orbital interaction sites are found as local minima on the AFIR function, providing approximate product structures. Such minimization paths, called AFIR paths, pass through corresponding approximate TS geometries. Thus, just by minimizing the AFIR function from many orientations, many reaction pathways can be obtained. Both approximate product and TS structures found along the AFIR paths are finally reoptimized without force by using a Quasi-Newton method. Thus, final optimized geometries are fully optimized true local minima and TSs.

Paths obtained by the AFIR minimizations depend on the initial orientation and the γ_{MIN} value, where the γ_{MAX} value is fixed at a given value and the search engine gradually increases γ value from γ_{MIN} to γ_{MAX}. Initial orientations and γ_{MIN} values are stochastically sampled in the standard algorithm (see ref 39 for details), and thus, γ_{MAX} is the only parameter to be set by users in the standard AFIR calculations and indicates an approximate upper limit of energy for the search. The initial orientation and the γ_{MIN} value can be chosen also by users if needed.

SMF-AFIR Method for MSX Search. In the SMF approach,[30] candidates of MSXs are explored at first by an automated reaction path search method such as the AFIR method as local minima on the following penalty function.

$$Y(\mathbf{Q}) = \frac{1}{2}[E^{\text{state1}}(\mathbf{Q}) + E^{\text{state2}}(\mathbf{Q})] + \frac{[E^{\text{state1}}(\mathbf{Q}) - E^{\text{state2}}(\mathbf{Q})]^2}{\alpha} \quad (2)$$

where $E^{\text{state1}}(\mathbf{Q})$ and $E^{\text{state2}}(\mathbf{Q})$ are PESs for the two crossing states and α is a constant parameter (in this study set to the standard value:[30] α = 30 kJ/mol). Once obtained, such candidates are reoptimized one-by-one using an accurate MSX optimization method such as the direct gradient (DG) method.[42] These two-step calculations using an automated reaction path search method are called by us SMF,[31,38] although similar penalty functions have previously been used in approximate MSX optimizations.[43,44]

In the present study, the AFIR method and the DG method were used in the first and second steps, respectively, (see ref 45 for our implementation of the DG method). In the present SMF-AFIR, at first the AFIR function $X(\mathbf{Q})$ is minimized with a given γ value, where $E(\mathbf{Q})$ in $X(\mathbf{Q})$ in eq 1 is replaced by $Y(\mathbf{Q})$ in eq 2. The SMF-AFIR leads to variety of MSX candidates along various associative reaction pathways. Once the AFIR minimization is converged, the full MSX optimization is performed without artificial force by using the DG method (see ref 38 for details). Thus, final optimized geometries are fully optimized MSXs without artificial force.

Geometrical Microiteration. The whole system is divided into two layers: the reaction center and the other. In the following, elements of gradient vectors concerned with reaction center (R) atoms and nonreaction center (N) atoms are denoted as g_i^R and g_n^N, respectively, and those of the Hessian matrix for the R−R block, the R−N coupling (C) block, and the N−N block are denoted as h_{ij}^R, h_{im}^C, and h_{nm}^N, respectively. In the microiteration technique, the geometrical subspace fulfilling $g_n^N = 0$ for all n is considered. In other words, positions of all nonreaction center atoms are optimized with fixing reaction center atoms before every geometrical displacement of reaction center atoms. This can significantly reduce the number of force calculations on reaction center atoms.[12,13] In general, reaction center and nonreaction center atoms are treated by QM and MM calculations, respectively, and thus, the microiteration technique can considerably reduce the number of QM calculations, as demonstrated below.

The microiteration technique can be easily combined with the AFIR method, just by modifying the code so that geometry optimization for positions of nonreaction center atoms is performed before every AFIR minimization step. The only complication is the treatment of Hessian matrix for the reaction center atoms. In practice, the following effective Hessian is used to account for couplings between two layers (see ref 46 for details).

$$\frac{\partial E(\mathbf{Q})}{\partial q_i \partial q_j} = h_{ij}^R - \sum_{3p}^{m}\sum_{3p}^{n} h_{im}^C W_{nm}^N h_{nj}^C \quad (3)$$

where q_i are coordinates of reaction center atoms, p is the number of nonreaction center atoms, and W_{nm}^N are elements of the inverse Hessian matrix of the N−N block. Obtaining the inverse matrix can be demanding when the size of the N−N block is large. The present enzyme contains more than 5000 nonreaction center atoms, and the size of the N−N block is as large as ∼15000 × 15000. Hence, we omitted elements for atoms distant more than 10 Å from reaction center atoms; a similar treatment was tested in ref 47.

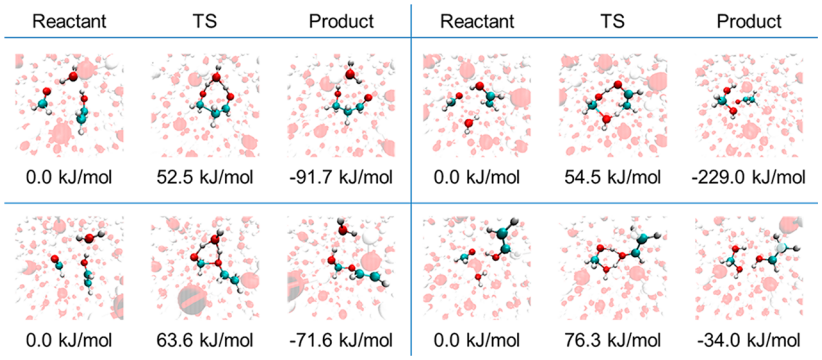

Figure 1. Four independent reaction pathways among $H_2CO + H_2C{=}C(H)OH + H_2O$ reactants in $(H_2O)_{299}$. Reactants, TSs, and products are fully optimized local minima, first-order saddles, and local minima, respectively, without artificial force, on the PES with the 2727 internal degrees of freedom.

Computation Details. As explained in ref 39, both function minimization and saddle point optimization were performed by the rational function optimization[48] method implemented in the GRRM program.[49] When a minimization step exceeded 0.5 Å, the step size is reduced to 0.5 Å by the trust radius[50] (TR) method, whereas the step size was controlled not to exceed 0.1 Å by the TR method in TS optimizations. The intrinsic reaction coordinate[51−56] (IRC) was computed starting from all obtained TSs using the quadratic algorithm.[54] In TS optimizations and IRC calculations, the Bofill's Hessian updating[57] method combining the SR1[58] and PSB[59] corrections was employed. In function minimizations, the Farkas and Schlegel's Hessian updating[2] scheme was employed combining the SR1 and BFGS[60−63] corrections by square root of the Bofill's parameter. The exact Hessian was calculated in every 50 minimization steps, in every 5 steps in TS optimizations, and in every 10 steps in IRC calculations. These are the default setups in the GRRM program.

In the present study, geometry displacements of reaction center atoms were treated by the GRRM program, whereas optimizations of positions of nonreaction center atoms were performed using the Gaussian 09 programs.[64] Energy values, gradient vectors, and Hessian matrices were calculated by the Gaussian 09 programs at given geometries. In the ONIOM calculations, reaction center atoms and others were treated by the B3LYP method with small basis sets and the AMBER force field[65] implemented in the Gaussian 09 programs, respectively.

3. NUMERICAL TESTS

Aldol Reaction in Water Cluster. The first test system of the microiteration AFIR method is a single water-catalyzed aldol reaction in $(H_2O)_{299}$ cluster, where the reaction center consisting of the two reactants, H_2CO and $H_2C{=}C(H)OH$, and the H_2O catalyst molecule were treated by the B3LYP/6-31G method and the $(H_2O)_{299}$ solvent cluster was treated with the AMBER force field. Although a similar calculation in the gas phase was done previously,[39] it was done again for comparison. In both $(H_2O)_{299}$ cluster and gas-phase calculations, the AFIR minimizations were performed starting from 100 random orientations with γ_{MAX} = 100 kJ/mol, where the fragments in the reaction center, $H_2CO + H_2C{=}C(H)OH + H_2O$, were at first randomly distributed and then 299 water molecules were randomly placed around the reaction center. After the AFIR minimizations, obtained approximate TSs and products were fully reoptimized, and IRCs were also computed from the fully optimized TSs. It should be noted that these calculations were performed just to show performance of the present method.

Figure 1 lists four pathways leading to four independent products obtained in the present search, where only the reaction center atoms are shown explicitly. It should be noted that the AFIR method predicted these pathways automatically using no initial guess associated with the reaction mechanisms. These four products correspond to the four independent products obtained in the gas-phase calculation. Table 1 shows the numbers of QM calculations required in the entire search including the AFIR minimizations, reoptimizations starting from approximate TSs and products, and IRC calculations, together with the numbers of independent paths. The number of QM calculations in $(H_2O)_{299}$ is comparable to (actually smaller than) in the gas phase, despite that there are as many as 2727 internal degrees of freedom in the former. The fact that the number of QM calculations is smaller in $(H_2O)_{299}$ is because the reaction center is more rigid in $(H_2O)_{299}$ than in the gas phase due to cage effects of the $(H_2O)_{299}$ cluster. This comparison demonstrates that the microiteration technique worked very well in the AFIR calculation.

Table 1. Numbers of QM-force and QM-Hessian Calculations Required in the Entire Search and the Numbers of Independent Paths Obtained by the AFIR Search[a]

	QM-force	QM-Hessian	no. of independent paths
in $(H_2O)_{299}$[b]	8707	241	4
in gas phase[c]	13 434	331	4

[a]Start from 100 random orientations with γ_{MAX} = 100 kJ/mol [b]ONIOM(B3LYP/6-31G:AMBER) [c]B3LYP/6-31G

Enzymatic Reaction. Another example of the microiteration AFIR method is an application to the first step in the catalytic mechanism of the isopenicillin N synthase (IPNS).[66,67] The mechanism of the entire multistep reaction has been well studied by both QM-only model calculations and ONIOM-(QM/MM) calculations.[14,68−70] Thus, this can be a good example to test the present method.

The ONIOM setup is completely the same as that used in the previous studies, where 65 including 4 link atoms are treated by the B3LYP method while the total of 5368 atoms is in MM calculation. The starting structure of the present AFIR search shown in Figure 2 is the septet end-on complex between O_2 and IPNS, which was prepared in the previous study based on an X-ray structure.[68] As stated above, our interest is finding

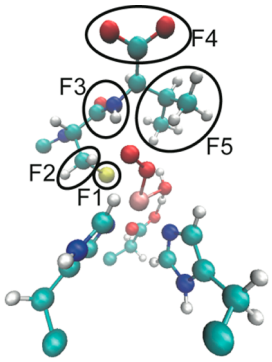

Figure 2. Reaction center in IPNS used in this study and fragmentation of the substrate into five functional and substitution groups.

reaction pathways involving local active sites for chemical bond reorganizations, and this initial structure can be a reasonable starting point to search for such pathways. Thus, we did not sample initial orientations by the stochastic search in the present application. Instead, the substrate molecule was divided systematically into five groups (F1−F5), as shown in Figure 2, and artificial forces were placed between the O_2 molecule and these fragments.

To speed up the calculations, smaller basis sets were employed in this study: LANL2DZ (basis function and effective core potential) on Fe and 3-21G* on others. Three spin-states, that is, triplet, quintet, and septet, were considered, as suggested in ref 69. In each spin-state, the AFIR functions for all O_2−F*n* pairs were minimized with γ_{MAX} = 100 kJ/mol and γ_{MIN} = 0 kJ/mol. Thus, this search is expected to find all reaction pathways with barriers lower than ∼100 kJ/mol. In SMF-AFIR calculations for triplet/quintet- and quintet/septet-MSXs, the γ value was fixed to 100 kJ/mol. A smaller value $\gamma = 0.75\gamma_R$ was also considered when bond rearrangement(s) occurred at least in one of the two spin states at $\gamma = \gamma_R$. When bond rearrangement(s) occurred both of the two spin states, a smaller γ_R was chosen. In other words, these calculations with two different γ values can find MSXs in both reactant and product valleys.

Figure 3 lists all obtained stationary points in the systematic search. F1 is reactive only on the quintet PES, and an O_2 insertion between S and Fe atoms takes place with a relatively low barrier (^{5}TS**1**/**2**: and ^{5}**2**). F2 is reactive on all the three states (^{3}**2**, ^{3}TS**1**/**2**, ^{5}**3**, ^{5}TS**1**/**3**, ^{5}**4**, ^{5}TS**3**/**4**, ^{7}**2**, and ^{7}TS**1**/**2**) and is the most reactive on the quintet PES. In these pathways, O_2 abstracts one of the H atoms in F2 giving −C(H)═S: or Fe−OO−H. Although there is no stationary point related to F3 in Figure 3, a proton transfer from NH in F3 occurred in all the three spin states during the AFIR minimizations. Geometry optimizations starting from these approximate products for F3 gave the reactant species on each spin state. This indicates that the proton transfer is easy but the species generated after the proton transfer is not stable at the present computation level. On the quintet PES, an O_2 detachment path was found in the AFIR minimization for O_2−F4 (^{5}**5**, ^{5}TS**1**/**5**, ^{5}**6**, ^{5}TS**5**/**6**). No reaction path was found with F5.

In the SMF-AFIR calculations with small $\gamma = 0.75\gamma_R$, MSXs ($^{3/5}$MSX1 and $^{5/7}$MSX1) in the reactant valley were found. In the reactant valley, spin multiplicity can change easily through these low energy MSXs, and the quintet state is the most preferable. In the product valley for the reaction involving F2, triplet−quintet transition may take place through $^{3/5}$MSX2, where $^{3/5}$MSX2 is slightly lower in energy than ^{3}**2** due to small

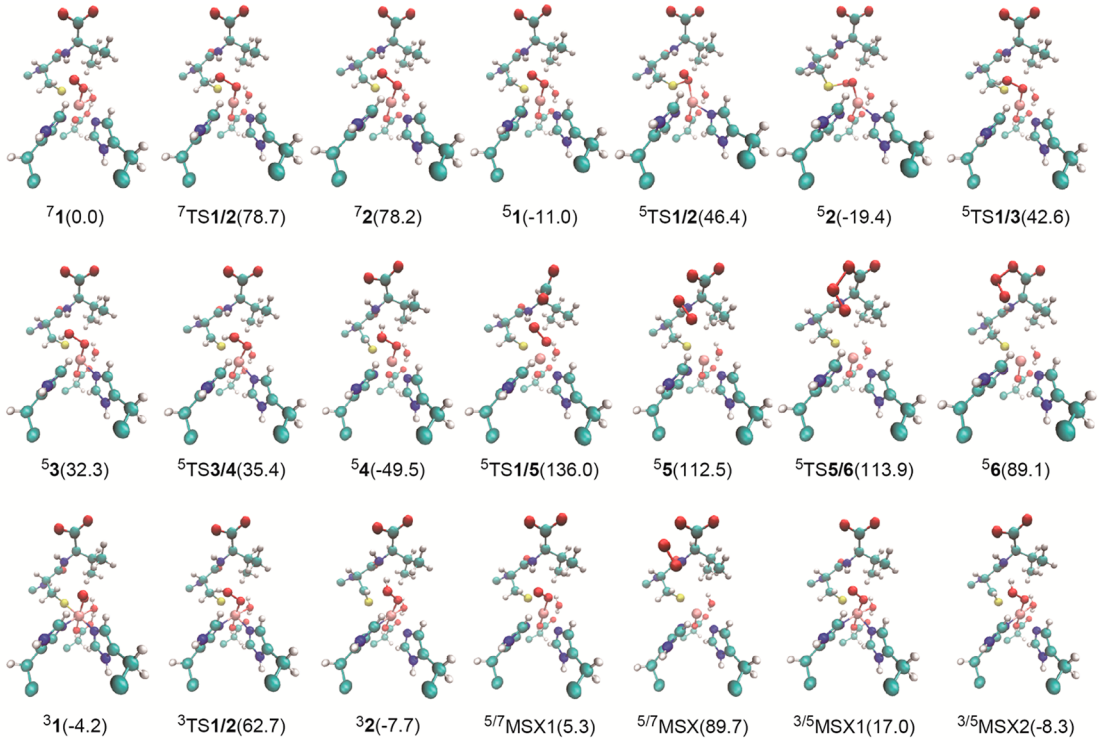

Figure 3. All obtained stationary structures for the initial step of the catalytic mechanism of IPNS. These are fully optimized local minima, first-order saddles (TSs), and minima on seam of crossing (MSXs) without artificial force, on the PES with the 16098 internal degrees of freedom (only the reaction center atoms are shown in this figure for clarity). Energies shown in parentheses are relative to ^{7}**1** in kJ/mol.

dx.doi.org/10.1021/ct300633e | J. Chem. Theory Comput. 2012, 8, 5058−5063

change in the protein conformation during the search. Another MSX outside the reactant valley is $^{5/7}$MSX2 for the O_2 detachment.

In total, 4764 QM-force and 623 QM-Hessian calculations were made in the entire search. For F2 and F4 on the quintet PES, pathways consisting of two steps were obtained by single AFIR minimizations. In these calculations, reoptimizations of approximate TSs obtained as the highest energy points along corresponding AFIR paths converged only to one of the two TSs for the two steps or did not converged. Even in such a case, one has both reactant and product geometries, respectively, as initial and terminal points of the corresponding AFIR path. Hence, the corresponding TSs can easily be obtained by one of interpolation methods.[5] In this study, these TSs (^{5}TS**1**/**3**, ^{5}TS**1**/**5**, and ^{5}TS**5**/**6**) were located by the double-end version of the GRRM method.[71,72] The total number of QM calculations shown above includes costs of these extra search.

The present results indicate that generation of ^{5}**4**, Fe−OO−H, is the most feasible channel. This is consistent with the mechanism proposed in the previous study.[14] Moreover, generation of ^{5}**2**, Fe−OO−S− species, is suggested as a minor channel. Further investigation of these and later steps using larger basis sets and the AFIR method will be published elsewhere. It should be emphasized that we did not use any initial guess about the reaction mechanism, except for the reactant structure. The only assumption we made was that the substrate can be divided into five functional and substitution groups, as shown in Figure 2. Dividing molecules into such groups can be done systematically. In other words, the present method will be very useful in finding reaction pathways that takes place within a small active site of the enzyme especially when the catalytic mechanism is largely unknown. Furthermore the present systematic search may be fully automatized in the future, providing an automatic search of the best reaction pathways in enzymatic reactions including explicitly the contribution of protein environments.

Discussions. We note that $(H_2O)_{299}$ or protein structures optimized in each microiteration are just a single local minimum. Barriers and reaction energies vary depending on their structures. For obtaining accurate energetics, one should use a method that samples many structures, such as the free-energy perturbation method,[73,74] especially when surrounding environments fluctuate dramatically. Combining AFIR with such a method is possible and can be a future subject.

A merit of the use of AFIR is that it can find not only the lowest one but also all low-lying pathways. In general, microiteration is much faster than such sampling methods. Thus, an efficient strategy can consist of two-stages: find all low-lying paths by the microiteration AFIR method, and then, examine important ones further by an expensive sampling method. Furthermore, some paths that are not important in a given enzyme may turn to have significance in a mutant. The present method can quickly explore possibilities of new channels that may be realized by a mutation.

4. SUMMARY

The AFIR method was combined with the ONIOM(QM/MM) method and the geometrical microiteration technique. In the microiteration-AFIR method, before taking every AFIR minimization step, positions of all MM atoms were optimized with fixed QM atom positions. Thus, the AFIR method explores the geometrical subspace fulfilling the condition that the force on the MM atoms equals to zero. Thus, the method is very efficient in searching reaction pathways that take place in a QM active site (typically consisting of tens of atoms) in a large MM environment. Numerical tests for an organic reaction in water cluster and for an enzymatic reaction demonstrated that the microiteration technique worked very well in the AFIR calculations. In the single water-catalyzed Aldol reaction in $(H_2O)_{299}$ cluster, the microiteration-AFIR method automatically found four independent reaction pathways obtained in the corresponding gas-phase calculation, where the number of QM-calculations was even smaller in the $(H_2O)_{299}$ cluster than in the gas phase. In the second example, that is, an application to the first step of the full catalytic mechanism of IPNS, the microiteration-AFIR method was able to locate 21 stationary structures without using any initial guess about the reaction mechanism and predicted the most preferable reaction path that was found previously on the basis of standard geometry ONIOM optimization calculations. The present method will be useful in systematic analysis and prediction of mechanisms of chemical reactions in very large environments such as protein and solution.

AUTHOR INFORMATION

Corresponding Author

*E-mail: smaeda@mail.sci.hokudai.ac.jp; keiji.morokuma@emory.edu.

Notes

The authors declare no competing financial interest.

ACKNOWLEDGMENTS

This work is partly supported by a grant from Japan Society for the Promotion of Science (Grants-in-Aid for Scientific Research (KAKENHI) No. 23685004) at Hokkaido University, a grant from Japan Science and Technology Agency with a Core Research for Evolutional Science and Technology (CREST) in the Area of High Performance Computing for Multiscale and Multiphysics Phenomena at Kyoto University, as well as a grant from U.S. AFOSR (Grant No. FA9550-10-1-0304) at Emory University. S.M. thanks Dr. Tsutomu Kawatsu of Institute for Molecular Science for providing the initial structure and the ONIOM setup for IPNS. S.M. thanks Mr. Ryohei Uematsu of Hokkaido University for helpful comments.

REFERENCES

(1) Schlegel, H. B. *J. Comput. Chem.* **1982**, *3*, 214−218.
(2) Farkas, Ö.; Schlegel, H. B. *J. Chem. Phys.* **1999**, *111*, 10806−10814.
(3) Schlegel, H. B. *J. Comput. Chem.* **2003**, *24*, 1514−1527.
(4) Jensen, F. Optimization techniques. *Introduction to Computational Chemistry*, 2nd ed.; Wiley: Chichester, 2007; pp 380−420.
(5) Schlegel, H. B. *WIREs Comput. Mol. Sci.* **2011**, *1*, 790−809.
(6) Warshel, A.; Levitt, M. *J. Mol. Biol.* **1976**, *103*, 227−249.
(7) Singh, U. C.; Kollman, P. A. *J. Comput. Chem.* **1986**, *7*, 718−730.
(8) Field, M. J.; Bash, P. A.; Karplus, M. *J. Comput. Chem.* **1990**, *11*, 700−733.
(9) Maseras, F.; Morokuma, K. *J. Comput. Chem.* **1995**, *16*, 1170−1179.
(10) Senn, H. M.; Thiel, W. *Angew. Chem., Int. Ed.* **2009**, *48*, 1198−1229.
(11) Chung, L. W.; Hirao, H.; Li, X.; Morokuma, K. *WIREs Comput. Mol. Sci.* **2012**, *2*, 327−350.
(12) Vreven, T.; Morokuma, K.; Farkas, Ö.; Schlegel, H. B.; Frisch, M. J. *J. Comput. Chem.* **2003**, *24*, 760−769.
(13) Vreven, T.; Frisch, M. J.; Kudin, K. N.; Schlegel, H. B.; Morokuma, K. *Mol. Phys.* **2006**, *104*, 701−714.

(14) Lundberg, M.; Kawatsu, T.; Vreven, T.; Frisch, M.; Morokuma, K. *J. Chem. Theory Comput.* **2009**, *5*, 222−234.
(15) Wales, D. J.; Scheraga, H. A. *Science* **1999**, *285*, 1368−1372.
(16) *Optimization in Computational Chemistry and Molecular Biology: Local and Global Approaches*; Floudas, C. A., Pardalos, P. M., Eds.; Kluwer Academic Publishers: Dordrecht, 2000.
(17) Dobson, C. M.; Šali, A.; Karplus, M. *Angew. Chem., Int. Ed.* **1998**, *37*, 868−893.
(18) Wales, D. J. *Int. Rev. Phys. Chem.* **2006**, *25*, 237−282.
(19) Dill, K. A.; Ozkan, S. B.; Shell, M. S.; Weikl, T. R. *Annu. Rev. Biophys.* **2008**, *37*, 289−316.
(20) Maddox, J. *Nature* **1988**, *335*, 201−201.
(21) Woodley, S. M.; Catlow, R. *Nat. Mater.* **2008**, *7*, 937−946.
(22) Bondensgård, K.; Jensen, F. *J. Chem. Phys.* **1996**, *104*, 8025−8031.
(23) Quapp, W.; Hirsch, M.; Imig, O.; Heidrich, D. *J. Comput. Chem.* **1998**, *19*, 1087−1100.
(24) Irikura, K. K.; Johnson, R. D., III *J. Phys. Chem. A* **2000**, *104*, 2191−2194.
(25) Müller, E. M.; de Meijere, A.; Grubmüller, H. *J. Chem. Phys.* **2002**, *116*, 897−905.
(26) Ohno, K.; Maeda, S. *Chem. Phys. Lett.* **2004**, *384*, 277−282.
(27) Maeda, S.; Ohno, K. *J. Phys. Chem. A* **2005**, *109*, 5742−5753.
(28) Ohno, K.; Maeda, S. *J. Phys. Chem. A* **2006**, *110*, 8933−8941.
(29) Ohno, K.; Maeda, S. *Phys. Scr.* **2008**, *78*, 058122.
(30) Maeda, S.; Ohno, K.; Morokuma, K. *J. Phys. Chem. A* **2009**, *113*, 1704−1710.
(31) Maeda, S.; Ohno, K.; Morokuma, K. *Adv. Phys. Chem.* **2012**, *2012*, 268124.
(32) Maeda, S.; Taketsugu, T.; Morokuma, K. *J. Phys. Chem. Lett.* **2012**, *3*, 1900−1907.
(33) Maeda, S.; Ohno, K. *J. Phys. Chem. A* **2007**, *111*, 4527−4534.
(34) Maeda, S.; Ohno, K. *J. Am. Chem. Soc.* **2008**, *130*, 17228−17229.
(35) Ohno, K.; Maeda, S. *J. Mol. Catal. A: Chem.* **2010**, *324*, 133−140.
(36) Maeda, S.; Morokuma, K. *J. Chem. Phys.* **2010**, *132*, 241102.
(37) Maeda, S.; Komagawa, S.; Uchiyama, M.; Morokuma, K. *Angew. Chem., Int. Ed.* **2011**, *50*, 644−649.
(38) Maeda, S.; Saito, R.; Morokuma, K. *J. Phys. Chem. Lett.* **2011**, *2*, 852−857.
(39) Maeda, S.; Morokuma, K. *J. Chem. Theory Comput.* **2011**, *7*, 2335−2345.
(40) Maeda, S.; Morokuma, K. *J. Chem. Theory Comput.* **2012**, *8*, 380−385.
(41) Collins, M. A. *Theor. Chem. Acc.* **2002**, *108*, 313−324.
(42) Bearpark, M. J.; Robb, M. A.; Schlegel, H. B. *Chem. Phys. Lett.* **1994**, *223*, 269−274.
(43) Ciminelli, C.; Granucci, G.; Persico, M. *Chem.—Eur. J.* **2004**, *10*, 2327−2341.
(44) Levine, B. G.; Coe, J. D.; Martínez, T. J. *J. Phys. Chem. B* **2008**, *112*, 405−413.
(45) Maeda, S.; Ohno, K.; Morokuma, K. *J. Chem. Theory Comput.* **2010**, *6*, 1538−1545.
(46) Maeda, S.; Ohno, K.; Morokuma, K. *J. Chem. Theory Comput.* **2009**, *5*, 2734−2743.
(47) Melaccio, F.; Olivucci, M.; Lindh, R.; Ferré, N. *Int. J. Quantum Chem.* **2011**, *111*, 3339−3346.
(48) Banerjee, A.; Adams, N.; Simons, J.; Shepard, R. *J. Phys. Chem.* **1985**, *89*, 52−57.
(49) Maeda, S.; Osada, Y.; Morokuma, K.; Ohno, K. *GRRM*, a developmental version. See http://grrm.chem.tohoku.ac.jp/SRPS/GRRMe.HTM (accessed date July 27, 2012) for the latest distributed version, GRRM11.
(50) Culot, P.; Dive, G.; Nguyen, V. H.; Ghuysen, J. M. *Theor. Chim. Acta.* **1992**, *82*, 189−205.
(51) Fukui, K. *J. Phys. Chem.* **1970**, *74*, 4161−4163.
(52) Ishida, K.; Morokuma, K.; Komornicki, A. *J. Chem. Phys.* **1977**, *66*, 2153−2156.
(53) Müller, K.; Brown, L. D. *Theor. Chim. Acta* **1979**, *53*, 75−93.
(54) Page, M.; McIver, J. W., Jr. *J. Chem. Phys.* **1988**, *88*, 922−935.
(55) Gonzalez, C.; Schlegel, H. B. *J. Chem. Phys.* **1989**, *90*, 2154−2161.
(56) Hratchian, H. P.; Schlegel, H. B. *J. Chem. Theory Comput.* **2005**, *1*, 61−69.
(57) Bofill, J. M. *J. Comput. Chem.* **1994**, *15*, 1−11.
(58) Murtagh, B. A.; Sargent, R. W. H. *Comput. J.* **1970**, *13*, 185−194.
(59) Powell, M. J. D. *Math. Program., Ser. A* **1971**, *1*, 26−57.
(60) Broyden, C. G. *J. Inst. Math. Appl.* **1970**, *6*, 76−90.
(61) Fletcher, R. *Comput. J.* **1970**, *13*, 317−322.
(62) Goldfarb, D. *Math. Comput.* **1970**, *24*, 23−26.
(63) Shanno, D. F. *Math. Comput.* **1970**, *24*, 647−656.
(64) Frisch, M. J.; Trucks, G. W.; Schlegel, H. B.; Scuseria, G. E.; Robb, M. A.; Cheeseman, J. R.; Scalmani, G.; Barone, V.; Mennucci, B.; Petersson, G. A.; Nakatsuji, H.; Caricato, M.; Li, X.; Hratchian, H. P.; Izmaylov, A. F.; Bloino, J.; Zheng, G.; Sonnenberg, J. L.; Hada, M.; Ehara, M.; Toyota, K.; Fukuda, R.; Hasegawa, J.; Ishida, M.; Nakajima, T.; Honda, Y.; Kitao, O.; Nakai, H.; Vreven, T.; Montgomery, Jr., J. A.; Peralta, J. E.; Ogliaro, F.; Bearpark, M.; Heyd, J. J.; Brothers, E.; Kudin, K. N.; Staroverov, V. N.; Kobayashi, R.; Normand, J.; Raghavachari, K.; Rendell, A.; Burant, J. C.; Iyengar, S. S.; Tomasi, J.; Cossi, M.; Rega, N.; Millam, J. M.; Klene, M.; Knox, J. E.; Cross, J. B.; Bakken, V.; Adamo, C.; Jaramillo, J.; Gomperts, R.; Stratmann, R. E.; Yazyev, O.; Austin, A. J.; Cammi, R.; Pomelli, C.; Ochterski, J. W.; Martin, R. L.; Morokuma, K.; Zakrzewski, V. G.; Voth, G. A.; Salvador, P.; Dannenberg, J. J.; Dapprich, S.; Daniels, A. D.; Farkas, O.; Foresman, J. B.; Ortiz, J. V.; Cioslowski, J.; Fox, D. J. *Gaussian 09*, Revision A.2; Gaussian, Inc.: Wallingford, CT, 2009.
(65) Cornell, W. D.; Cieplak, P.; Bayly, C. I.; Gould, I. R.; Merz, K. M., Jr.; Ferguson, D. M.; Spellmeyer, D. C.; Fox, T.; Caldwell, J. W.; Kollman, P. A. *J. Am. Chem. Soc.* **1995**, *117*, 5179−5197.
(66) Baldwin, J. E.; Bradley, M. *Chem. Rev.* **1990**, *90*, 1079−1088.
(67) Schenk, W. A. *Angew. Chem., Int. Ed.* **2000**, *39*, 3409−3411.
(68) Lundberg, M.; Morokuma, K. *J. Phys. Chem. B* **2007**, *111*, 9380−9389.
(69) Lundberg, M.; Siegbahn, P. E. M.; Morokuma, K. *Biochemistry* **2008**, *47*, 1031−1042.
(70) Kawatsu, T.; Lundberg, M.; Morokuma, K. *J. Chem. Theory Comput.* **2011**, *7*, 390−401.
(71) Maeda, S.; Ohno, K. *Chem. Phys. Lett.* **2005**, *404*, 95−99.
(72) Maeda, S.; Ohno, K. *J. Chem. Phys.* **2006**, *124*, 174306.
(73) Hu, H.; Yang, W. *Annu. Rev. Phys. Chem.* **2008**, *59*, 573−601.
(74) Kosugi, T.; Hayashi, S. *J. Chem. Theory Comput.* **2012**, *8*, 322−334.